European Laboratory for Particle Physics

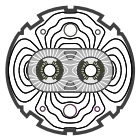

Large Hadron Collider Project

LHC Project Report 1082

Effect of phase advance between interaction points in the LHC on the beam-beam interaction

W. Herr, CERN, AB Department, CH-1211 Geneva 23
D. Kaltchev, TRIUMF, Vancouver, B.C. Canada

Abstract

Starting from the results from a large scale simulation campaign, we investigated the effects of the phase advance between beam-beam interactions for different configurations of the collision scheme. We have developed tools to study these effects qualitatively and quantitatively and in particular we have studied whether certain phase advances can enhance or suppress resonances. Conditions for the suppression of resonances have been derived.

Geneva, 1 April 2008

1 Introduction

It is well known that in the case of localized perturbations in a circular machine an appropriate choice of the phase between the perturbations can lead to the suppression or enhancement of resonances.
In this respect the symmetry and periodicity properties of the machine are all important [1]. The periodicity of the LHC collision points are shown in Fig. 1. The left figure shows

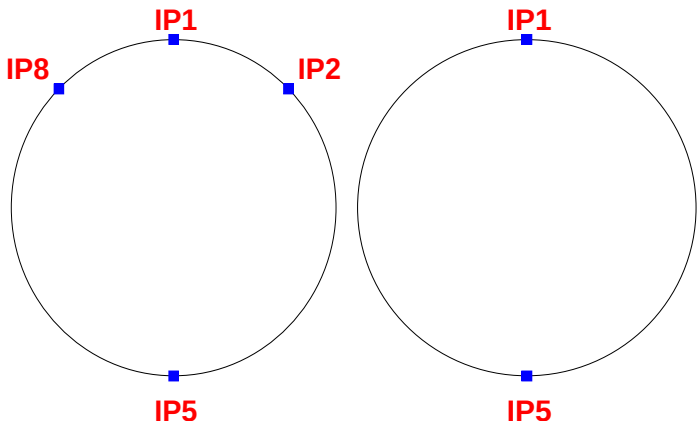

Figure 1: LHC collision points: left nominal, right two high luminosity collision points

the positions of the four nominal interaction points and the right figure shows only the two high luminosity points where the effects of parasitic beam-beam interactions are important. This choice was made to profit from partial compensation of first order beam-beam effects, in particular to minimize so-called PACMAN effects [2, 3].

An optimization of the collision scheme was made with a large scale tracking campaign [4].
Part of this study was aimed at finding a good working points for the machine when beams are colliding. The dynamic aperture was evaluated for different configurations and different angles in the x-y plane. Details on the procedure and the results can be found in [4]. To find a good working point for the machine the horizontal and vertical tunes have been varied and the dynamic aperture was computed for every step. The dynamic aperture shown here is defined as the minimum amplitude at which the particle is lost for 10^5 turn and for all seeds. The results of such a tune scan is shown in Fig. 2. In the horizontal tune we find two regions where the dynamic aperture is reduced to significantly smaller values and we identify these with resonances near $q_x = 4/13$ and $q_x = 5/16$ (q is the fractional part of the tune).
One of the crucial questions asked was whether these resonances can be suppressed or reduced by choosing a phase advance of $\frac{\pi}{2}$ between IP1 and IP5 [5]. Such a requirement would constrain the optical layout of the machine.
We present an analytical model to answer this question and compare to a simulation. In a second part we discuss a more general concept for resonance suppression and the necessary conditions, in particular whether these conditions can be met in the LHC.

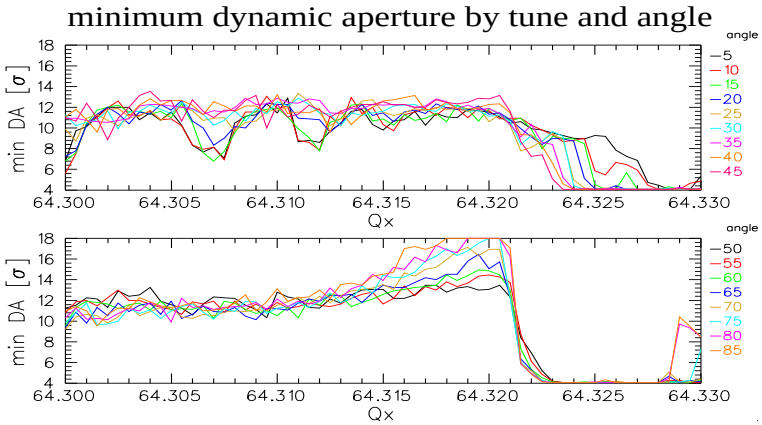

Figure 2: Tune scan showing resonances. The dynamic aperture in units if the beam size is plotted as a function of the horizontal tune and for different angles in the x-y plane.

2 Analytical treatment

2.1 Classical approach

A standard treatment to assess non-linear perturbations is the s-dependent Hamiltonian and perturbation theory:

$$\mathcal{H} \;=\; \mathcal{H}_0 + \delta(s)\epsilon V \tag{1}$$

where $\mathcal{H}_0$ is the unperturbed part of the Hamiltonian and ϵV describes the perturbation caused at the position s, specified by the δ function. The mathematical treatment is rather involved and in most cases cannot be carried beyond leading order in the perturbation. This can easily lead to wrong conclusions, which can still be found in the literature (e.g. 4th order resonance cannot be driven by sextupoles) and one must ask the question whether this is the most appropriate tool to deal with this problem. In the case of isolated non-linearities caused by very local beam-beam interactions we favour a map based approach as promoted by Dragt [6, 7] and described in details by Forest [8].

2.2 Approach using Lie transforms and invariant

In this approach the ring is represented by a finite sequence of maps, which describe the individual elements. Possible representations of these maps are Taylor maps and Lie maps [9].

In this study we shall use the Lie maps which are always symplectic and other advantages will become obvious. This technique allows to derive invariants of the motion in a straightforward way, in particular the extension of the results to multiple beam-beam interactions becomes an easy task.

To answer the initial question this is particularly relevant since we want to investigate the effect of the number of interaction points and the relative phase advance on the beam dynamics.

In the first part we derive the formulae for a single interaction point and later extend the method to multiple beam-beam interactions.

2.2.1 Single interaction point

The derivation for a single interaction point can be found in the literature (a particularly nice derivation by Chao [9]).

In this simplest case of one beam-beam interaction we can factorize the machine in a linear transfer map $e^{:f_2:}$ and the beam-beam interaction $e^{:F:}$, i.e.:

$$e^{:f_2:} \cdot e^{:F:} = e^{:h:} \tag{2}$$

with

$$f_2 = -\frac{\mu}{2}(\frac{x^2}{\beta} + \beta p_x^2) \tag{3}$$

where μ is overall phase, i.e. the tune Q multiplied by 2π, and β is the β-function at the interaction point. The function $F(x)$ corresponds to the beam-beam potential[1)]

$$F(x) = \int_0^x dx' f(x') \tag{4}$$

For a Gaussian beam we use for f(x) the well known expression for round beams:

$$f(x) = \frac{2Nr_0}{\gamma x}(1 - e^{\frac{-x^2}{2\sigma^2}}) \tag{5}$$

Here N is the number of particles per bunch, r_0 the classical particle radius, γ the relativistic parameter and σ the transverse beam size.
For the analysis we examine the invariant h which determines the one-turn-map (OTM) written as a Lie transformation $e^{:h:}$. The invariant h is the effective Hamiltonian for this problem.
As usual we transform to action and angle variables A and Φ, related to the variables x and p_x through the transformations:

$$x = \sqrt{2A\beta}\sin\Phi, \qquad p_x = \sqrt{\frac{2A}{\beta}}\cos\Phi \tag{6}$$

With this transformation we get a simple representation for the linear transfer map f_2:

$$f_2 = -\mu A \tag{7}$$

The function $F(x)$ we write as Fourier series:

$$F(x) \Rightarrow \sum_{n=-\infty}^{\infty} c_n(A) e^{in\Phi} \tag{8}$$

with the coefficients $c_n(A)$:

$$c_n(A) = \frac{1}{2\pi}\int_0^{2\pi} e^{-in\Phi} F(x) d\Phi \tag{9}$$

For the evaluation of (9) see [9]. We take some useful properties of Lie operators (any textbook [8, 9]):

$$:f_2:g(A) = 0, \qquad :f_2:e^{in\Phi} = in\mu e^{in\Phi}, \qquad g(:f_2:)e^{in\Phi} = g(in\mu)e^{in\Phi} \tag{10}$$

[1)] For a discussion of the Lie representation as a generalized kick map see [9].

and the CBH-formula for the concatenation of the maps (any textbook [8, 9]):

$$e^{:f_2:}\, e^{:F:} \;=\; e^{:h:} \;=\; \exp\left[: f_2 + \left(\frac{: f_2 :}{1 - e^{-:f_2:}}\right) F + \mathcal{O}(F^2) :\right] \tag{11}$$

which gives immediately for h:

$$h = -\mu A + \sum_n c_n(A) \frac{in\mu}{1 - e^{-in\mu}} e^{in\Phi}$$

$$\text{and} \qquad h = -\mu A + \sum_n c_n(A) \frac{n\mu}{2\sin(\frac{n\mu}{2})} e^{(in\Phi + i\frac{n\mu}{2})} \tag{12}$$

Away from resonances a normal form transformation gives:

$$h \;=\; -\mu A + c_0(A) \;= const. \tag{13}$$

On resonance, i.e. for the condition:

$$Q = \frac{p}{n} = \frac{\mu}{2\pi} \tag{14}$$

and with $c_n \neq 0$ we have:

$$\sin(\frac{n\pi p}{n}) = \sin(p\pi) \equiv 0 \qquad \forall \;\; integer \quad p$$

and the invariant h diverges. This is a well known result and not surprising.

2.2.2 Two interaction points

To study two interaction points we use a configuration as shown in Fig. 3 and extend the treatment of a single beam-beam interaction in [9] to any number of beam-beam interactions. Following the LHC conventions we label the interaction points IP1 and IP5. The phase advance between IP1 and IP5 is μ_1, from IP5 to IP1 it is μ_2 and the overall phase advance for one turn is $\mu \;=\; \mu_1 + \mu_2$. For the computation we have now

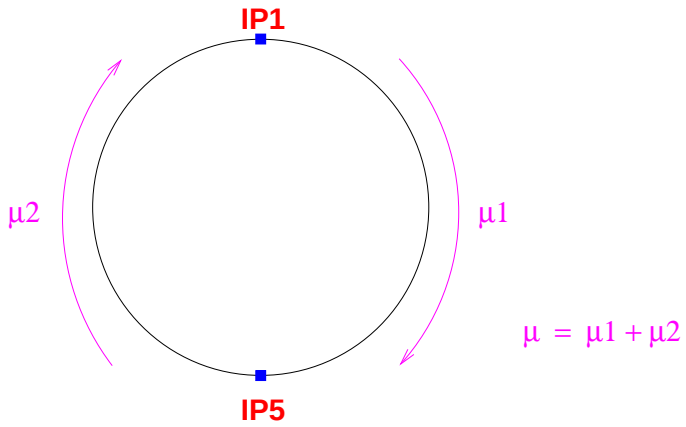

Figure 3: Two collision points with unequal phase advance.

two transfers f_2^1, f_2^2 and two beam-beam kicks F^1, F^2, assuming the first interaction point

(IP5) at μ_1, and the second (IP1) at μ [10]. The one turn map with the four transforms is then:

$$= \; e^{:f_2^1:}\, e^{:F^1:}\, e^{:f_2^2:}\, e^{:F^2:} \; = \; e^{:h_2:} \tag{15}$$

This we can easily re-write using the properties of Lie operators as:

$$\begin{aligned} &= \; e^{:f_2^1:}\, e^{:F^1:}\, e^{-:f_2^1:}\, e^{:f_2^1:}\, e^{:f_2^2:}\, e^{:F^2:} \; = \; e^{:h_2:} \\ &= \; e^{:f_2^1:}\, e^{:F^1:}\, e^{-:f_2^1:}\, e^{:f_2:}\, e^{:F^2:}\, e^{-:f_2:}\, e^{:f_2:} = \; e^{:h_2:} \\ &= \; e^{:e^{-:f_2^1:}F^1:}\, e^{:e^{-:f_2:}F^2:}\, e^{:f_2:} = \; e^{:h_2:} \end{aligned}$$

Assuming now the simplification;

$$f_2 \; = \; -\mu A, \quad f_2^1 \; = \; -\mu_1 A, \quad and \quad f_2^2 \; = \; -\mu_2 A \tag{16}$$

and remember that $g(:f_2:)e^{in\Phi} = g(in\mu)e^{in\Phi}$, we have:

$$e^{:f_2^1:}e^{in\Phi} \; = \; e^{in\mu_1}e^{in\Phi} \; = \; e^{in(\mu_1+\Phi)} \tag{17}$$

we find that the Lie transforms of the perturbations are phase shifted (see e.g. [8]). Therefore:

$$e^{:e^{-:f_2^1:}F^1:}\, e^{:e^{-:f_2:}F^2:}\, e^{:f_2:} = \; e^{:h_2:} \tag{18}$$

becomes simpler with substitutions of $\Phi_1 \; \rightarrow \; \Phi + \mu_1$ and $\Phi \; \rightarrow \; \Phi + \mu$ in the functions G^1 and G:

$$e^{:G^1(\Phi_1):}e^{:G(\Phi):}e^{:f_2:} \quad \Rightarrow \qquad e^{:G^1(\Phi_1)+G(\Phi):}e^{:f_2:} \tag{19}$$

This reflects the phase shifted distortions and we get for h_2:

$$h_2 = -\mu A + \sum_{n=-\infty}^{\infty} \frac{n\mu c_n(A)}{2\sin(n\frac{\mu}{2})} \left[e^{-in(\Phi+\mu/2+\mu_1)} + e^{-in(\Phi+\mu/2)}\right] \tag{20}$$

or re-written as[2)]:

$$h_2 = -\mu A + 2c_0(A) + \underbrace{\sum_{n=2}^{\infty} \frac{2n\mu c_n(A)}{\sin(n\frac{\mu}{2})} \cos\left[n(\Phi + \frac{\mu}{2} + \frac{\mu_1}{2})\right] \cos(n\frac{\mu_1}{2})}_{\text{interesting part}} \tag{21}$$

Nota bene, because of:

$$e^{:F(\Phi):}e^{:f_2:} \quad \rightarrow \quad e^{:G^1(\Phi_1)+G(\Phi):}e^{:f_2:} \tag{22}$$

the above treatment can be generalized to more interaction points, in particular including long range interactions.
In practice the equation (21) is evaluated to a maximum order N, in our case up to order 40. We get:

$$h_2 = -\mu A + 2c_0(A) + \underbrace{\sum_{n=2}^{N} \frac{2n\mu c_n(A)}{\sin(n\frac{\mu}{2})} \cos\left[n(\Phi + \frac{\mu}{2} + \frac{\mu_1}{2})\right] \cos(n\frac{\mu_1}{2})}_{\text{interesting part}} \tag{23}$$

with $N = 40$.

[2)] For head on collisions only $c_n(A)$ for even orders in n are non-zero and the sum needs to be done only for even terms

2.2.3 Comparison with numerical model

To test our result, we compare the invariant h to the results of a particle tracking program [10].

The model we use in the program is rather simple:

- linear transfer between interactions
- beam-beam kick for round beams
- compute action $I = \frac{\beta^*}{2\sigma^2}(\frac{x^2}{\beta^*} + p_x^2\beta^*)$
- compute phase $\Phi = \arctan(\frac{p_x}{x})$
- compare I with h as a function of the phase Φ

The evaluation of the invariant (12) is done numerically with Mathematica. The compar-

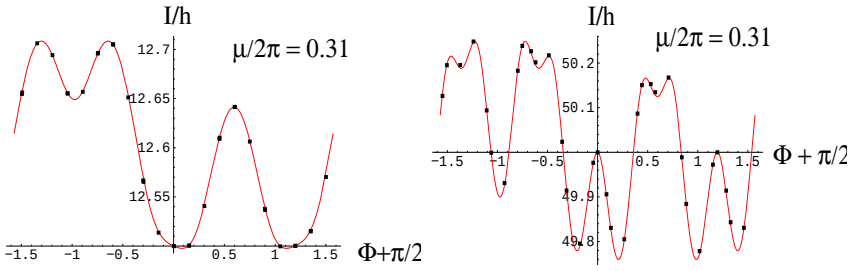

Figure 4: Comparison: numerical and analytical model for one interaction point. Shown for $5\sigma_x$ and $10\sigma_x$. Full symbols from numerical model and solid lines from invariant (12).

ison between the tracking results and the invariant h from the analytical calculation is shown in Fig.4 in the (I,Φ) space. Only one interaction point is used in this comparison and the particles are tracked for 1024 turns. The symbols are the results from the tracking and the solid lines are the invariants computed as above. The two figures are computed for amplitudes of 5 σ and 10 σ. The agreement between the models is excellent. The analytic calculation was again done up to the order N = 40. Using a lower number, the analytic model can reproduce the envelope of the tracking results, but not the details. Another comparison is done in Fig.5 for the case of two interaction points. The symbols

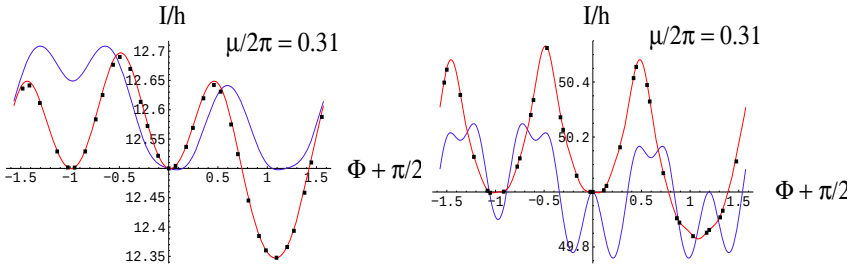

Figure 5: Comparison: numerical and analytical model for two interaction points. Shown for $5\sigma_x$ and $10\sigma_x$. Full symbols from numerical model and solid lines from invariant. Shown here are the invariant for one (eq. (12), blue line, not passing through the full symbols) and two (eq. (21), red line, passing through the full symbols) interactions to demonstrate the difference and the agreement with the tracking program.

are again from the simulation and the solid lines from the computation. For comparison the invariant for a single interaction point is included to demonstrate the difference. Again the agreement is excellent and shows the validity of the results.

2.3 Behaviour near a resonance

To show the behaviour of the system near a resonance, we show the invariant together with the tracking results near the 3rd order resonance in Fig. 6. It is clearly

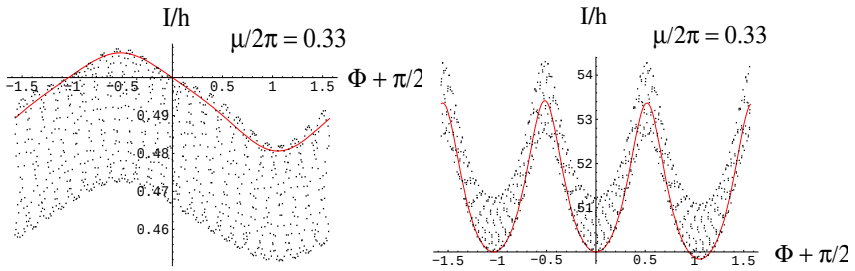

Figure 6: Comparison: numerical and analytical model for two interaction points on a resonance (3rd order).

demonstrated that the simulation differs quantitatively from the computed invariant at resonant tunes.

2.4 Analysis of the invariant

To analyse the behaviour of the invariant h near resonances, we examine the trigonometric part of the invariant.

$$h_2 \approx \sum_n 2n\mu c_n(A) \cdot \frac{\cos(n\frac{\mu_1}{2})}{\sin(n\frac{\mu}{2})} \cdot \cos(n(\Phi + \frac{\mu}{2} + \frac{\mu_1}{2})) \tag{24}$$

It can be easily seen that for phase advance $\mu_1/2\pi = 0.25 \cdot k$, where k is an integer and n divisible by 4 the invariant remains resonant.
However it remains finite under the condition: $n = 2\cdot$ (odd integer). We can therefore conclude that the resonance q = 4/13 could be suppressed by choosing the phase advance of $\frac{\pi}{2}$ between the two interaction points IP1 and IP5. The resonance for 5/16 does not fulfill this condition. This is demonstrated in Figs. 7 and 8. Here we show the logarithm of the trigonometric factor in equation (23) as a function of the tune $\mu/2\pi$ for $\mu_1/2\pi = 0.2604$ (Fig. 7) and for $\mu_1/2\pi = 0.2500$ (Fig. 8). The sum is again taken up to N=40. In this figure we ignore that some resonances may be absent when $c_n(A)$ is zero and demonstrate only the effect of the phase advance. While in the Fig. 7 all resonances are visible where the denominator becomes zero, in the second case with $\mu_1/2\pi = 0.2500$ many of the resonances are suppressed.
Another demonstration is shown in Figs. 9 and 10. In these figures we change the overall tune $\mu/2\pi$ in small steps and show the simulation results together with the invariant. In Fig. 9 the phase advance between the two interaction points is kept constant at $\mu_1/2\pi = 0.2604$. A phase advance of exactly $\mu_1/2\pi = 0.2500$ is used in Fig. 10.
The result is very clear: in Fig. 9 at the tunes of the resonances of 13th and 16th order the two models disagree. In the second case shown in Fig. 10 the discrepancies near the 13th order resonance have disappeared, i.e. it is suppressed by the choice of the phase advance and the invariant remains finite. This is in full agreement with the expectation from the analysis presented above. It is therefore impossible to suppress both resonances simultaneously with this simple condition.

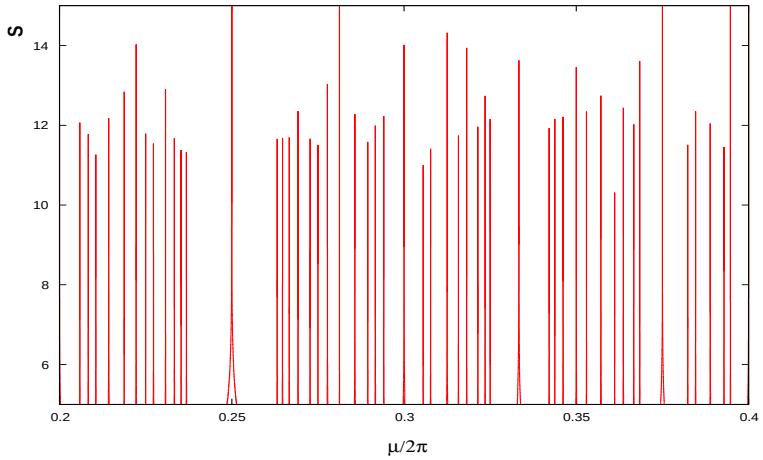

Figure 7: Resonance factor as function of tune $\mu/2\pi$ for $\mu_1/2\pi = 0.2604$.

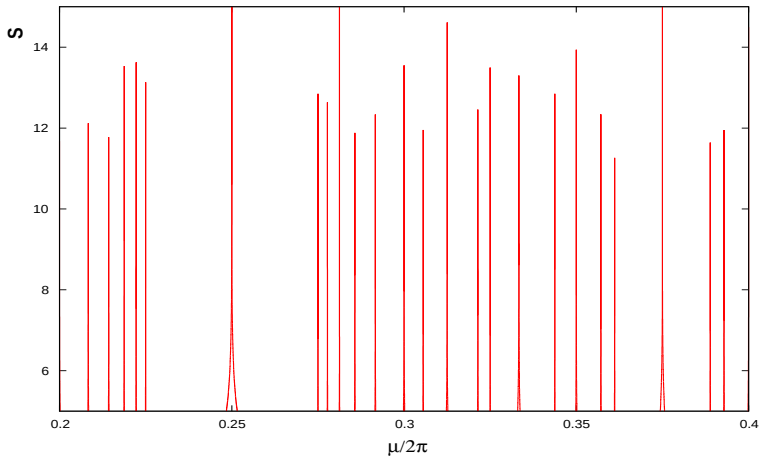

Figure 8: Resonance factor as function of tune $\mu/2\pi$ for $\mu_1/2\pi = 0.2500$.

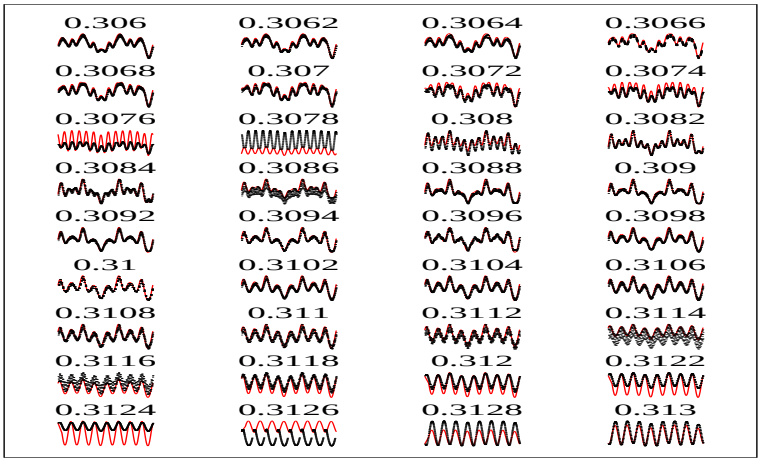

Figure 9: Comparison between numerical model and invariant for different values of the tune. For $\mu_1/2\pi = 0.2604$.

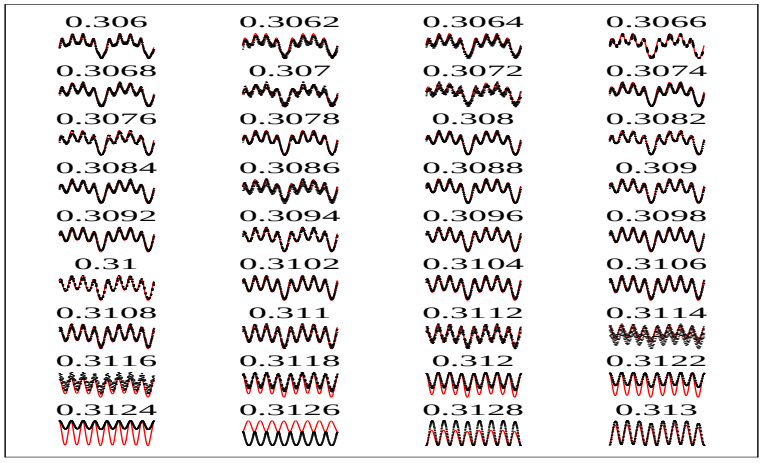

Figure 10: Comparison between numerical model and invariant for different values of the tune. For $\mu_1/2\pi = 0.2500$.

2.5 Required precision on the phase advance

Provided the correct conditions for a resonance suppression can be fulfilled, one needs to answer the question what precision is needed for these phase advances, i.e. for $\mu_1 = \frac{\pi}{2}$?
An answer is shown in Figs. 11 to 12. We analyse the equation (21) and show it for increasing deviation from the exact and ideal phase advance of $\mu_1 = \frac{\pi}{2}$. From these

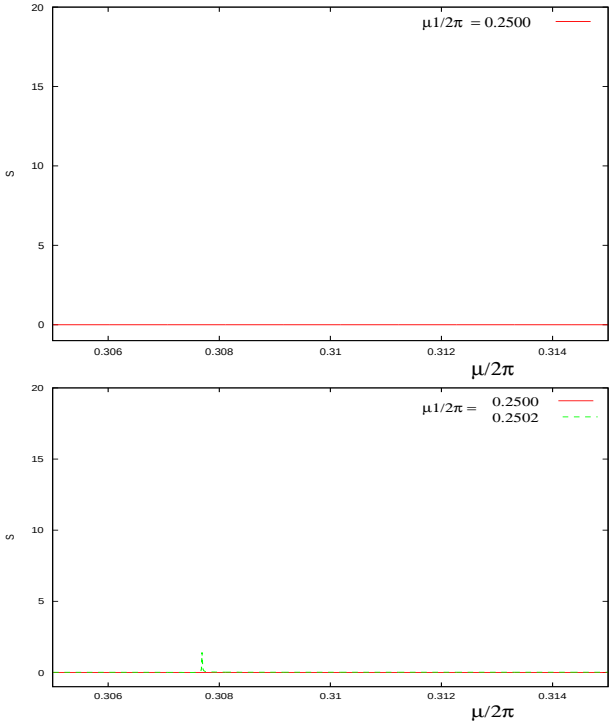

Figure 11: Perfect cancellation for $\mu_1 = \frac{\pi}{2}$ (left) and phase advance error of 0.0002 (right).

figures one can determine that an absolute phase error of more than 0.001 can already inhibit the suppression effect. It is therefore rather doubtful whether one can rely on this feature in practice, in particular in the presence of additional interaction points and PACMAN effects [2, 3].

2.6 Symmetry and periodicity

To answer the questions on the effect of phase advance between beam-beam interactions on the excitation of resonances we have full confidence in our method and in the case of a few interaction points we can immediately derive the necessary conditions from (12) or (21). Extending the method to many interactions (e.g. at N interaction points at azimuth Θ_i, not equally spaced), it becomes difficult to interpret the results directly. We follow a second approach [1] to get a qualitative and partially quantitative picture. The invariant can also be found in a form like [1]:

$$h \approx (Q - \frac{p}{n})A + N \cdot \xi \cdot U(A) + S \cdot V_n(A) \cdot \cos(n\Phi) \tag{25}$$

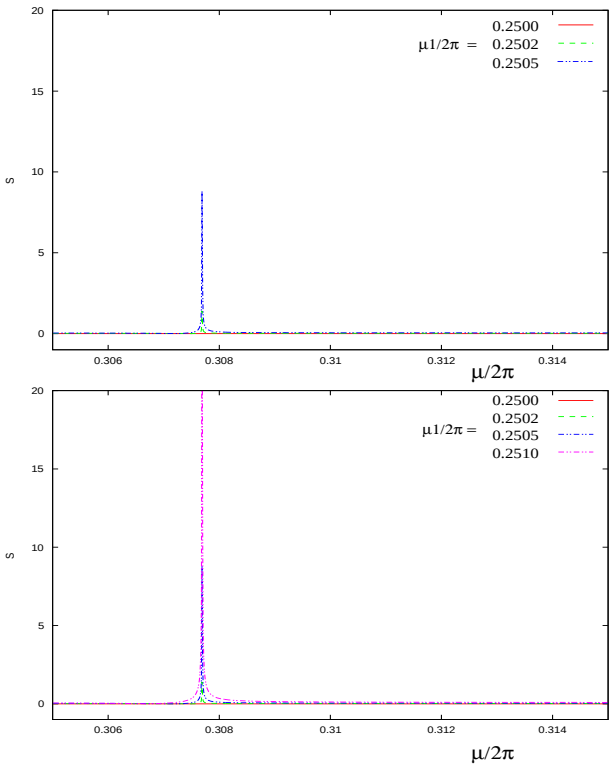

Figure 12: Phase advance error of 0.0005 (left) and 0.0010 (right).

where $V_n(A)$ is the resonant term and S describes the periodicity and can be re-written as:

$$S = \sqrt{(\sum_{i=1}^{N} \cos(p \cdot \Theta_i))^2 + (\sum_{i=1}^{N} \sin(p \cdot \Theta_i))^2} \tag{26}$$

(Θ_i is the azimuthal position of the ith beam-beam interaction, p is azimuthal harmonic) This gives us a Fourier decomposition of the resonant driving term.

2.6.1 The symmetric case

We start with a fully symmetric machine with two interaction points (Fig. 13). In the Figs. 14 and 15 we show the resonance suppression factor for a fully symmetric machine with two interaction points without phase errors. It can be seen that by an appropriate choice of the tune (phase advance between the two interaction points) the 16th order resonance, corresponding to the 1029th harmonic can be exactly cancelled (Fig.14). However for the same tune the 13th order resonance is enhanced (Fig.15).
In practice the collision pattern is not exactly symmetric (phase errors, additional interactions etc.) and the suppression is never complete, if possible at all.
The same suppression factor as in Fig. 15 is shown in Fig. 16, however this time the phases μ_1 and μ_2 differ by a small amount (0.0002). This rather small phase error is sufficient to destroy the suppression completely. It is now not possible to find any harmonic where the cancellation is complete.
The condition for four symmetric interaction points is shown in Fig. 17. The large number of suppressed harmonics make this is very interesting configuration (in theory).

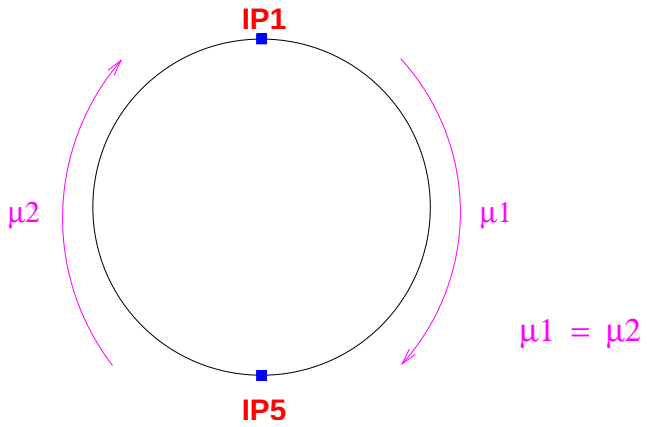

Figure 13: LHC collision scheme for two symmetric interaction points.

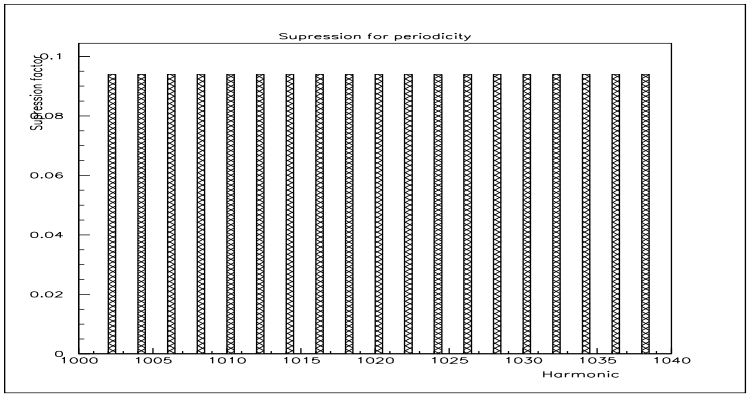

Figure 14: Resonance suppression factor for two symmetric interaction points. Around harmonic for 16th order.

2.6.2 The LHC case

In the nominal LHC we have four interaction regions but the conditions are much less favourable than in the case shown in Fig. 17:

- The interaction regions do not show a four-fold symmetry
- The phase advances between interaction regions are not multiple of Q/8 but non-regular
- Long range beam-beam interactions disturb the phase relationships
- PACMAN effects cause different phase advances between interaction points for different bunches
- Bunch to bunch fluctuations further disturb the phase between interaction points

The effect of the non-regular phase between the four interaction points is shown in Fig. 18. The pattern of S is not regular and non of the harmonics is completely suppressed. This effects is further enhanced when long range interactions are included (Fig.19). These and additional effects have been analysed in [1] in more detail.

As an observation from Figs. 17 and 19 and the analysis of the invariant one must also conclude that depending on the configuration and machine imperfections some harmonics can be strongly enhanced and will change the sensitivity of the machine to the tune significantly. The control of the tune and the possible correction of imperfections is highly desirable.

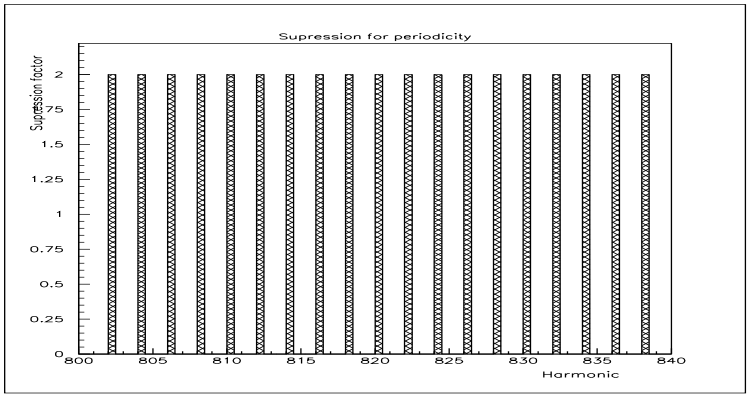

Figure 15: Resonance suppression factor for two symmetric interaction points. Around harmonic for 13th order.

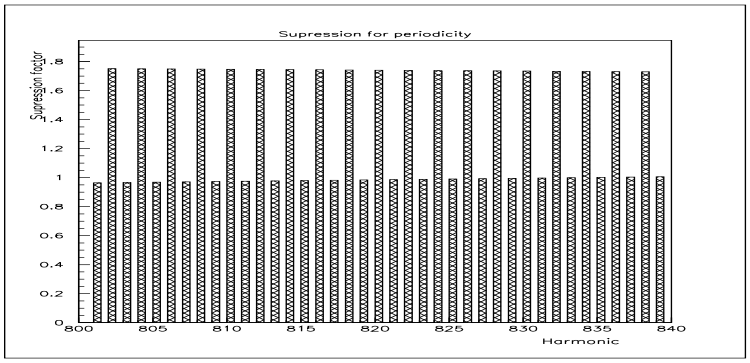

Figure 16: Resonance suppression factor for two symmetric interaction points with phase advance error.

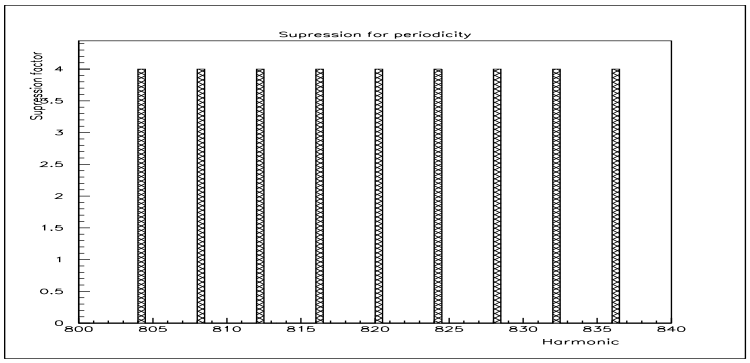

Figure 17: Resonance suppression factor for four symmetric interaction points.

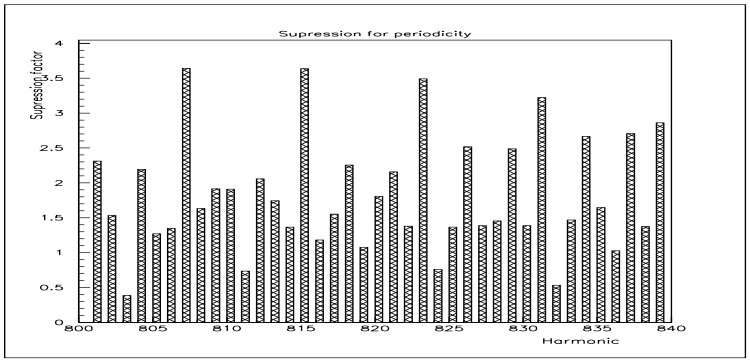

Figure 18: Resonance suppression factor for four LHC interaction points and nominal optics.

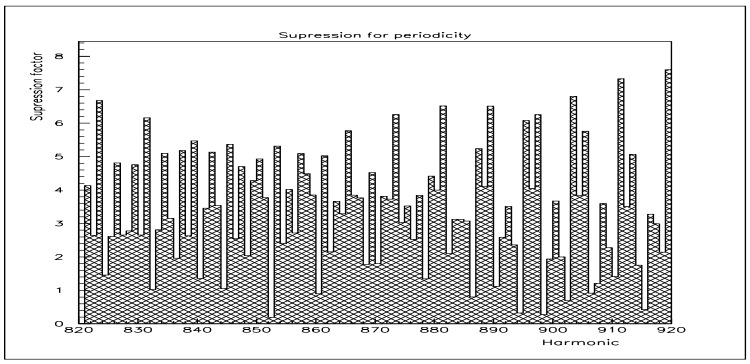

Figure 19: Resonance suppression factor for four LHC interaction points with head-on and long range interaction.

3 Summary

The results of our study we can summarize as follows:

- We have developed tools to study quantitatively the effect of phase advance relationships between multiple beam-beam interaction points.
- Only under certain and tight conditions individual resonances can be suppressed.
- A phase advance of $\pi/2$ between interaction points IP1 and IP5 is not required since the expected advantages are marginal and only of theoretical interest.
- Although it is always possible to define configurations where some resonances can be suppressed, such a suppression is unlikely to be useful in practice.
- Certain phase advances (e.g. caused by phase errors) may strongly enhance some resonances and must be corrected as needed.

References

[1] W. Herr, *Consequences of Periodicity and Symmetry for the Beam-Beam Effects in the LHC*, LHC Project Report 49 (1996).

[2] W. Herr, *Features and implications of different LHC crossing schemes*, LHC Project Report 628 (2003).

[3] W. Herr, *Effect of PACMAN bunches in the LHC*, LHC Project Report 39 (1996).

[4] W. Herr, E. McIntosh and F. Schmidt, CERN, D. Kaltchev, TRIUMF, Vancouver, Canada, *Large Scale Beam-beam Simulations for the CERN LHC Using Distributed Computing* Proc. EPAC 2006, Edinburgh 2006 (2006), page 528.

[5] T. Risselada, ABP-LCU section meeting, 29.01.2007.

[6] A. Dragt, *A Method of Transfer Maps for Linear and Non-linear Beam Elements*, IEEE Trans.Nucl.Science, Vol.NS-26, No 3, 1979.

[7] A. Dragt, *Analysis of the beam-beam interaction using transfer maps*, Proceedings of the Beam-beam Interaction Seminar, SLAC 1980, SLAC-PUB-2624 (1980).

[8] E. Forest, *Beam Dynamics, A New Attitude and Framework*, Harwood Academic Publishers 1998.

[9] A. Chao, *Lecture Notes on Topics in Accelerator Physics*, SLAC, March 2001.

[10] D. Kaltchev, *On beam-beam resonances observed in LHC tracking*, TRI-DN-07-9, TRIUMF, 2007.